Journal of Power Sources 260 (2014) 43–49

Contents lists available at ScienceDirect

Journal of Power Sources

journal homepage: www.elsevier.com/locate/jpowsour

In-situ temperature measurement in lithium ion battery by transferable flexible thin film thermocouples

Madhu Santosh K. Mutyala [a,1], Jingzhou Zhao [b,1,2], Jianyang Li [c], Hongen Pan [b,3], Chris Yuan [d], Xiaochun Li [e,*]

[a] Department of Electrical and Computer Engineering, University of Wisconsin-Madison, 1001 Mechanical Engineering Building, 1513 University Ave, Madison, 53706, USA
[b] Department of Mechanical Engineering, University of Wisconsin-Madison, 1001 Mechanical Engineering Building, 1513 University Ave, Madison, 53706, USA
[c] Department of Mechanical Engineering, University of Wisconsin-Milwaukee, EMS 725, 3200 North Cramer Street, Milwaukee, WI 53211, USA
[d] Department of Mechanical Engineering, University of Wisconsin-Milwaukee, EMS 1019, 3200 North Cramer Street, Milwaukee, WI 53211, USA
[e] Department of Mechanical Engineering, University of Wisconsin-Madison, 1035 Mechanical Engineering Building, 1513 University Ave, Madison, 53706, USA

HIGHLIGHTS

- Temperature inside pouch cell captured *in-situ* by flexible thin film thermocouples.
- Sensors are fabricated and transferred onto current collector of the cell.
- Sensor assembly process is minimally intrusive and semi-automated.
- Method presented hold promise to be implemented in battery management systems.

ARTICLE INFO

Article history:
Received 17 October 2013
Received in revised form
16 February 2014
Accepted 3 March 2014
Available online 13 March 2014

Keywords:
Lithium ion battery
Thin film sensor
Flexible substrate
Battery management system

ABSTRACT

Temperature monitoring is important for improving the safety and performance of Lithium Ion Batteries (LIB). This paper presents the feasibility study to insert flexible polymer embedded thin film thermocouples (TFTCs) in a lithium ion battery pouch cell for *in-situ* temperature monitoring. A technique to fabricate polyimide embedded TFTC sensors on glass substrates and later transfer it onto thin copper foils is presented. The sensor transfer process can be easily integrated into the assembly process of a pouch cell, thus holding promise in implementing in Battery Management Systems (BMS). Internal temperature of the LIB pouch cell was measured *in-situ* when the sensor embedded battery was operated at high rate charge–discharge cycles. The polyimide embedded TFTCs survived the battery assembly process and the battery electrolyte environment. It is observed that the heat generation inside the battery is dominant during the high-rate of discharges. The developed technique can serve to improve the battery safety and performance when implemented in battery management systems and enhance the understanding of heat generation and its effects.

* Corresponding author. Present address: Department of Mechanical and Aerospace Engineering, University of California, Los Angeles, 48-121G Engineering IV, 420 Westwood Plaza, Los Angeles, CA 90095, USA. Tel.: +1 310 825 2383; fax: +1 310 206 4805.
E-mail addresses: mmutyala@wisc.edu (M.S.K. Mutyala), jzhao53@wisc.edu, frankzz8000@ucla.edu (J. Zhao), jianyang@uwm.edu (J. Li), Hpan27@wisc.edu, panhg@njcit.cn (H. Pan), cyuan@uwm.edu (C. Yuan), xcli@engr.wisc.edu, xcli@seas.ucla.edu (X. Li).
[1] First authors.
[2] Present address: Department of Mechanical and Aerospace Engineering, University of California, Los Angeles, 43-119 Engineering IV, 420 Westwood Plaza, Los Angeles, CA 90095, USA.
[3] Permanent address: Department of Mechanic and Electronic Engineering, Nanjing College of Information Technology, 99 Wen Lan Road, Nanjing 210046, China.

http://dx.doi.org/10.1016/j.jpowsour.2014.03.004
0378-7753/

1. Introduction

Lithium Ion Batteries (LIBs), after dominating the consumer market of portable electronics, are now entering the transportation sector and have already been installed on some of the latest generation of electric and hybrid electric vehicles (EV and HEV) and even passenger planes. Yet challenges still exist in thermal related safety and performance issues, rendering the importance of battery thermal management undisputed [1]. Implementing *in-situ* monitoring of temperature inside individual lithium ion battery cells in Battery Management Systems (BMS) holds great promise in improving the safety of a pack by allowing earlier detection of the onset of thermal runaway, which can lead to rupture, fire or even explosion of the cell [1–4]. Non-intrusive sensing of the temperature at critical locations inside the battery is desirable for validation of many modeling and simulation works that imply the presence of considerable temperature gradient inside a battery cell during operation [5–10].

Existing internal temperature monitoring techniques either lack the desired spatial resolution or are not compatible with the standard battery cell assembly processes. Forgez et al. measured the internal temperature of a $LiFePO_4$/graphite lithium-ion battery (26650 cylindrical cell) by destructively inserting a commercial thermocouple with a junction of 1 mm in diameter into the cell in an argon protected atmosphere [6]. Srinivasan et al. developed a four-probe technique that allows for the internal temperature, more precisely the anode temperature of the cell, being monitored externally without an extra internal sensor [4,11,12]. This method can potentially be easily implemented in BMS to realize internal temperature monitoring of individual cells. An intrinsic relationship was found between the impedance change of the cell and its internal temperature. Measuring the phase shift between an applied sinusoidal current and the resulting voltage gives the temperature information. The observed relationship was attributed to the SoC (state-of-charge)-independence and the temperature-dependence of the impedance of the solid-electrolyte-interphase (SEI) layer formed on the graphite, rendering this method only applicable so far to lithium ion batteries with graphite anode. And it only gives reliable measurement under the condition that the properties of the SEI layer stays unchanged. Furthermore, it treats all anode layers as one unit and measures the average temperature. Modified methods are thus developed by Schmidt et al. [13] and Raijmakers et al. [14] and they do not restrict their application to the temperature sensitivity of the SEI. Lee et al. integrated micro thin film resistance temperature detectors (RTD) into the lithium ion secondary battery for *in-situ* temperature monitoring [15–17]. The thin film sensors were encapsulated in Parylene and inserted into a spirally-wound lithium ion pouch cell. Since the sensor is flexible while the resistance of the RTD sensor is both temperature- and strain-dependent, this coupling effect may affect the accuracy of the measurement. Moreover, little information is given regarding whether the sensor was inserted into the cell during or after the cell assembly process and how. Li et al. experimentally investigated the temporal and spatial variations of internal temperature of a large-format laminated battery by inserting 12 commercial thermocouples into the cell [18]. The sensors were placed inside the battery before sealing of the cell but are apparently obtrusive.

In this work, a novel method is developed to fabricate and transfer flexible TFTCs onto the battery current collector and then embed in lithium ion pouch cells for *in-situ* internal temperature measurement. Key requirements listed below for minimally-intrusive sensing inside a prismatic lithium ion battery pouch cell were identified and met.

1. Transport or transfer of lithium ions between electrodes may not be affected due to the presence of the sensor.
2. The sensor film may not react with or dissolve in the battery electrolyte.
3. The sensor has to be compatible with the pouch cell assembly process.

The novel thin film sensor transfer technique developed was to overcome the difficulty of direct fabrication of multilayered thin film sensors onto rough, flexible and metal substrate. K-type TFTCs encapsulated in polyimide was fabricated on a glass substrate using conventional microfabrication techniques. As-fabricated sensor film was released from the substrates and then conformally bonded to the copper current collector of the battery. Cured polyimide is

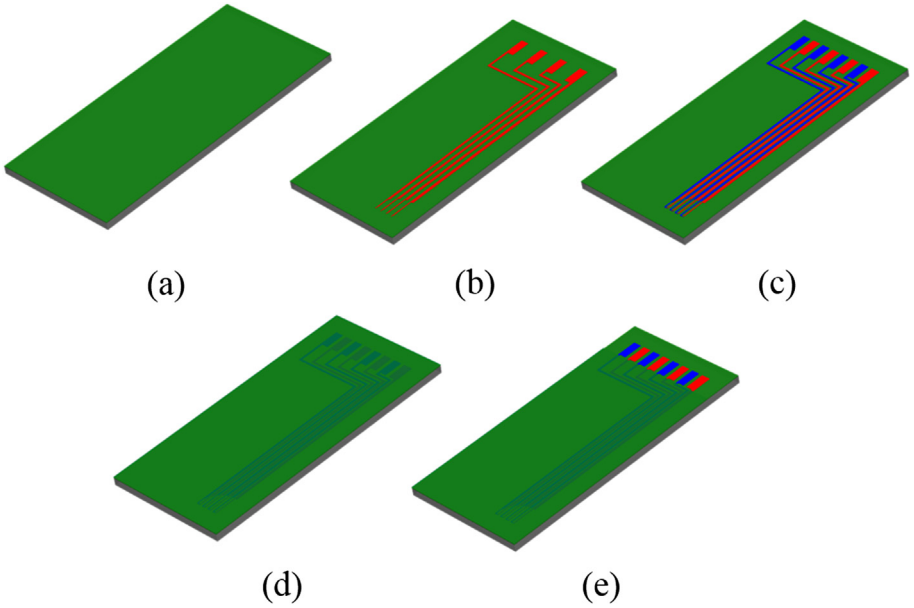

Fig. 1. TFTC Fabrication process: (a) microscopy glass slide spin coated with PI-2545 and cured, (b) thin film of Ti/alumel deposited on cured PI, (c) deposition of Ti/chromel, (d) TFTC encapsulated by spin coating another layer of PI-2545, (e) exposing the contact pads by dissolving the uncured coated PI using MF321 developer.

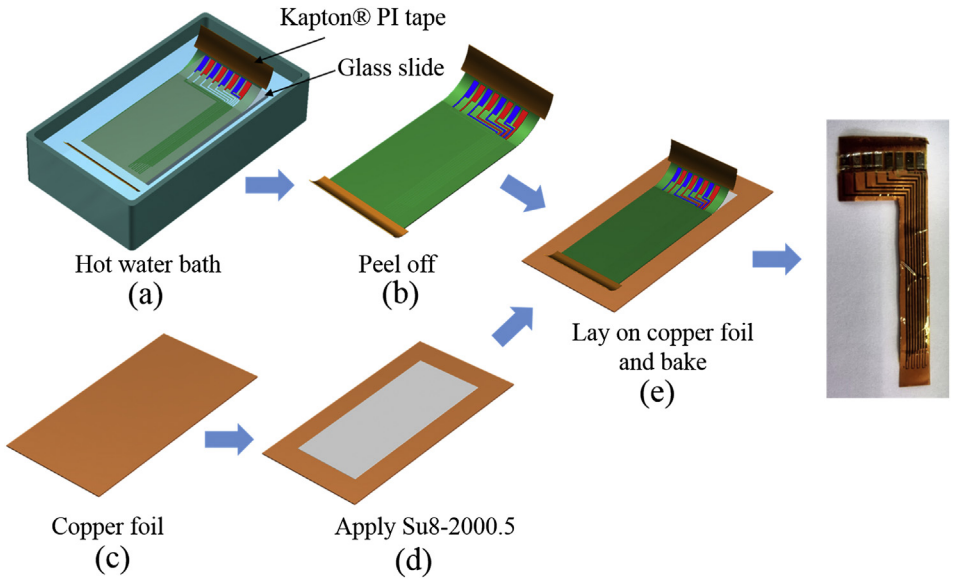

Fig. 2. (a) Kapton® PI tape applied to the edges of PI embedded TFTC, (b) setup immersed in warm water bath to peel off PI embedded TFTC, (c, d, e) Peeled off TFTC transferred to SU8 2000.5 coated copper foil.

known as insoluble in polar aprotic solvents [19] which are typically used in lithium ion battery electrolytes. TFTCs have much smaller junction sizes than thin film RTDs offering a higher spatial resolution. They are not sensitive to strain induced resistance change as opposed to thin film RTDs. The finished sensor was attached to one side of the stacked battery electrode inside the cell where there is minimum flow of lithium ions. And this procedure can be easily incorporated into any standard pouch cell assembly process. The TFTC sensor embedded inside the pouch cell successfully captured the internal transient temperature change at high charging and discharging rates.

2. Sensor fabrication and transfer

Flexible TFTCs were fabricated on microscopy glass slides functioning as the working substrate. High temperature compatibility, smooth surface finish, and inexpensiveness of microscopy glass slides, makes it an ideal substrate for PI based thin film devices. Polyimide was selected as the flexible substrate due to its superior dielectric property as well as its chemical and thermal stability at temperature up to 400 °C. The glass slides were precleaned using acetone, IPA and rinsed with DI water followed by N_2 blow and heat drying. The microscopy glass slides were spin coated with PI-2545 (HD Microsystems) and soft baked at 90 °C for 2 min. The PI coated slides were then placed in a programmable polymer convection oven and cured in nitrogen gas ambience. Curing of the PI is done by heating the samples from room temperature to 200 °C at a ramp rate of 4 °C min^{-1}. Temperature is maintained at 200 °C for 30 min. Samples are again subjected to heating from 200 °C to 350 °C at a rate of 4 °C min^{-1}. Temperature is again held at 350 °C for 1 h followed by cool down process till the system achieves room temperature. After the curing is complete, we obtain a thin film (~2–3 μm thick) of PI stuck to the glass slide.

K-type thermocouple consisting of thin films of alumel (Ni/Al/Si/Mn) and chromel (Ni/Cr) is used as a temperature sensing element. Alumel and chromel thin films are deposited using DC sputtering (CVC 601 system). Standard photolithography and liftoff process is followed while pattering the thin films. The sputtering system is vacuumed to a base pressure of <2e-6 torr. Alumel deposition is performed using 3″ alumel target at 500 W power for 20 min in an Ar plasma at a pressure of 5 mT and 20 sccm Ar flow rate. Alumel deposition is followed by liftoff technique in acetone bath to get the patterned electrodes. Chromel deposition is done using 3″ chromel target at 500 W power for 23 min in Ar plasma at a pressure of 5 mT. Thin film of Ti (~5 nm) is used as the adhesion layer between PI and alumel/chromel metal films. Fig. 1(a–c) shows the schematic of TFTC fabrication on cured PI surface.

The TFTC is encapsulated by spin coating another layer of PI-2545. The sample is then soft baked for 2 min at 90 °C. The electrode pads for connection to the terminal box are revealed by exposing the electrode pads using MF321 developer. The developer dissolves the uncured PI and uncovers the electrode pads. Later, the PI encapsulated samples are again cured using the curing process mentioned before. TFTC fabrication and encapsulation is followed by transferring it onto copper foil. Fig. 2(a–c) shows the schematic of the transfer process. PI encapsulated TFTC staged on the glass slide is immersed in warm (~75 °C) water bath. Since, glass is hydrophilic in nature it allows the water to seep into the PI–Glass interface there by letting the PI embedded TFTC peel off. However, the residual stress in this thin film system causes it to roll inwards leading the TFTC to curl onto itself. This is overcome by holding the edges of the PI embedded TFTC using Kapton® PI tape. The released TFTC is laid on SU8 2000.5 coated thin copper foil and soft baked for

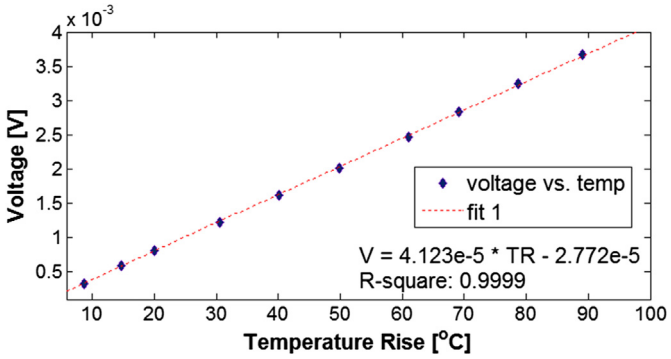

Fig. 3. Calibration curve of PI embedded TFTC sensor showing the output voltage against the temperature rise.

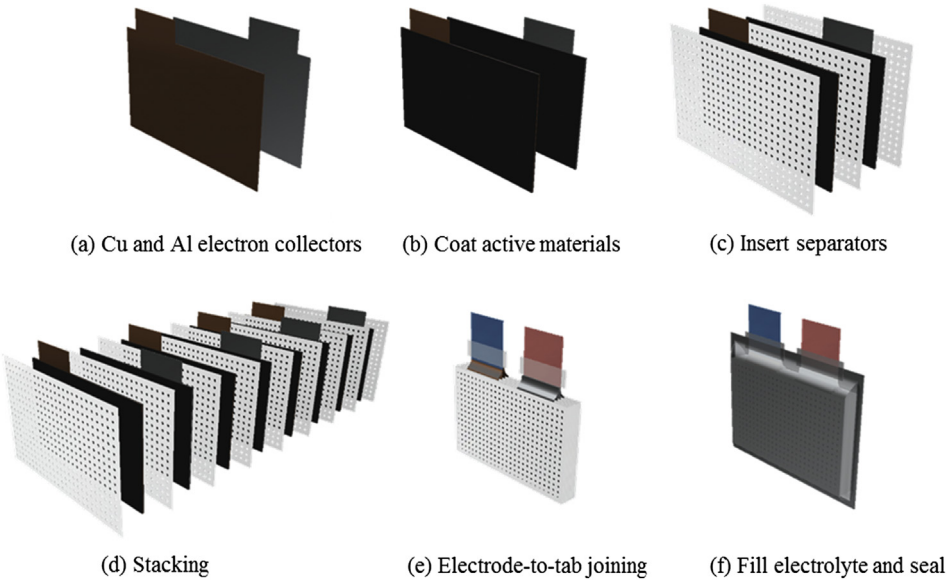

Fig. 4. Schematic of the assembly process of a LIB pouch cell.

5 min at 90 °C and later cured at ~150 °C for 30 min. This process leads to the successful transfer of PI embedded thin film systems onto metallic surfaces, metal foils and other unconventional substrates on which direct fabrication of thin film systems is unfavorable. Fig. 2(e) shows the picture of PI embedded TFTC unit being transferred to thin copper foil.

3. Sensor characterization

The electrical characterization of the sensor unit was performed by measuring the sensor unit's output voltage when it was subjected to a unit temperature rise. A programmable Thermo Scientific Lindberg/Blue-M model box furnace was used as the heat source during sensor calibration. A standard K-type thermocouple wire, attached under the sensor unit was used as a reference unit. The terminal box (SCB-68) used with the data acquisition (DAQ) system was placed sufficiently far from the heat source in order to experience negligible deviation from the ambient temperature. The temperature of the heat source was increased in step increment of 10 °C till 100 °C. Measurements were made after the temperature was stabilized after each step increment. The output of the K-type thermocouple wire was associated to the voltage produced by the sensor unit to extract the Seebeck coefficient. The calibration curve shown in Fig. 3 specifies the sensitivity of the thin film sensor unit to be ~41.2 μV °C^{-1}. The sensitivity of the PI embedded TFTC closely matches the thermoelectric sensitivity of the commercial K-type thermocouple wire used as the reference unit.

4. PI embedded flexible TFTC assembly into LIB pouch cell

Once the sensor was ready, it was taken into a dry room and assembled with a 3 Ah pouch cell. The schematic of the assembly process of a typical pouch cell without sensor is shown in Fig. 4.

The copper and aluminum current collectors, as shown in Fig. 4(a), are coated with graphite (anode) and $LiNi_{1/3}Mn_{1/3}Co_{1/3}O_2$ (cathode) respectively on both sides as shown in Fig. 4(b). Multilayered electrodes and separators are stacked as shown in Fig. 4(d). The electrodes are then welded to the battery tabs followed by

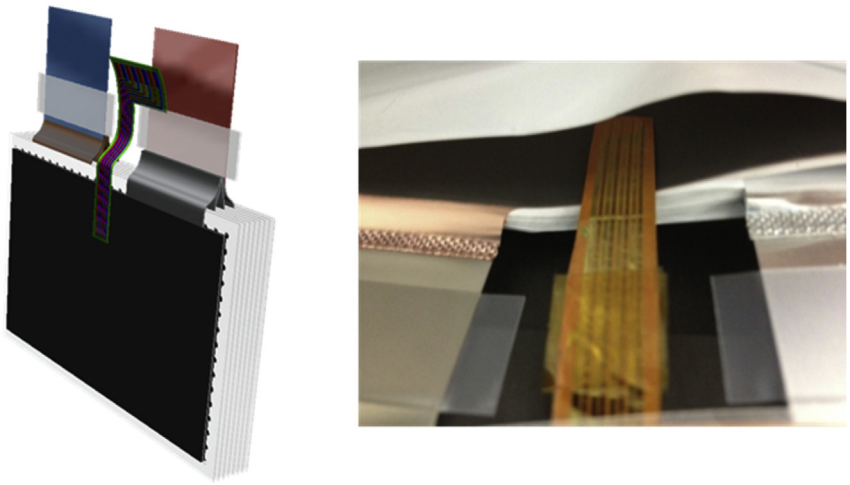

Fig. 5. Positioning of sensors.

Fig. 6. Pouch cell with embedded flexible TFTC sensor.

sealing into an aluminum laminated film case filled with electrolyte (1.0 M LiPF6 in ethylene carbonate (EC) and ethyl-methyl carbonates (EMC) (7:3)), as shown in Fig. 4(e & f). The flexible sensor was attached to the stacked electrodes after step Fig. 4(e) as shown in Fig. 5. The sensor pads are exposed the same way as the copper and aluminum electrodes. Fig. 6 shows the completed pouch cell with flexible TFTC sensor embedded and connection pads exposed.

The insertion of the sensor into the battery cell was conducted in a semi-automated manner by adding just one step to an existing battery cell assembly line, thus is robust and repeatable. Compared to other methods reported in the literature, this method does not require alteration or destruction of the cell. Instead, sensor geometry can be tailored according to the geometry of an existing pouch cell.

5. Battery testing, temperature measurement results and discussion

A schematic of the experimental setup is shown in Fig. 7. Chromel and alumel wires were bonded to the exposed pads on the flexible sensor by conductive silver paste and connected to the DAQ box for *in-situ* temperature measurement and data collection. A commercial thermocouple (Omega Engineering) is attached to the laminated aluminum film for reference temperature measurement. Much care was taken to make sure the commercial sensor and TFTC overlap in the thickness direction of the cell.

The as-prepared pouch cell was cycled on ARBIN BT-2000 battery test system (Arbin, USA) at the charge/discharge rate of 3 C (9 A), 5 C (15 A), and 7 C (21 A) cycles between 2.7 V and 4.2 V at room temperature after an initial discharge at 1 C (3 A). Table 1 shows the charge/discharge capacity and energy with step-increased C rates. Temperature measured from both sensors was being logged while the cell was being charged and discharged as shown in Fig. 8. TFTC inside the battery reliably measures the cell temperature evolution and little temperature difference is found between TFTC and the reference TC due to the fact that they are only separated by a 150 μm thick aluminum laminated film which is a good thermal conductor.

The temperature evolution characteristics result from the heat generation during charging and discharging of the cell at step-increased C-rates. To further investigate the heat generation characteristics during cell operation, current and voltage profiles are plotted respectively together with temperature in Figs. 9 and 10. Temperature profile is first related to the heat generation rate by a semi-quantitative analysis. Then the relationship of current and voltage with the heat generation rate is discussed.

Lumped capacitance assumption is used and the lithium cell is assumed to have uniform temperature measured by the TFTC. The heat generated by the cell is transferred through air at room temperature which can be considered as a constant temperature sink. The heat generation rate q can thus be estimated using an energy balance on the battery as follows [20]

$$q = MC_p\frac{dT}{dt} + hA(T - T_{air})$$

The first term on the right side of the equation is the amount of heat stored inside the battery and the latter is the heat transferred

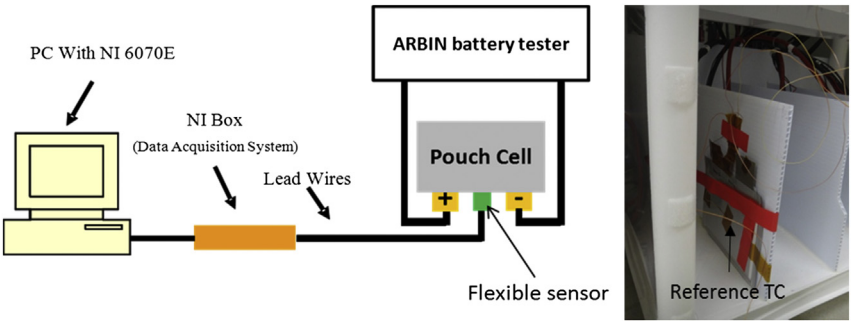

Fig. 7. Experimental setup for *in-situ* temperature measurement in LIB.

Table 1
Charge/discharge capacity and energy at step-increased C-rates.

C-rate	Charge capacity [Ah]	Discharge capacity [Ah]	Charge energy [kW]	Discharge energy [kW]
1 C	/	2.91	/	10.39
3 C	2.76	2.52	11.14	8.47
5 C	2.52	2.15	10.43	6.99
7 C	2.28	1.76	9.6	5.38

from the surface of the battery to the constant temperature surroundings. $(T - T_{air})$ is the temperature rise of the cell which is measured by TFTC at any instance.

According to the energy balance analysis, the magnitude of heat generation rate is larger when both temperature rise and its rate of increase is larger. This thus leads to the conclusion that, within each cycle of same C-rate, discharge phase generates thermal energy faster than charge phase, as evidenced by the larger slope and value of the temperature rise in each discharge period as shown in Fig. 9.

A general trend of higher temperature rise at higher C-rate can also be observed, with an exception for the 7 C charging. This is because the maximum charging voltage is set at 4.2 V to avoid over charge which make the 7 C charging period much shorter than other cycles as can be seen in the current profile in Fig. 9. Even though the heat generation rate during 7 C charging is expected to be larger than those of 5 C and 3 C, it is terminated too soon thus less thermal energy is released than needed to allow for a substantial temperature rise.

Abrupt changes in heat generation rate reflected in the abrupt changes of slope are observed for all discharge temperature curves, which all happen near the substantial voltage drops that happen before the end of each constant current discharge phase as shown in Fig. 10. Similar observation can be found in the literature indicating a change on the sign of the acceleration of the phenomena inside the electrode [21].

The results clearly show that the embedded flexible TFTC sensors can reliable measure temperature inside the lithium ion battery cell and survived the battery assembly process showing no adverse effects like electrolyte leakage, battery puffing, internal shorting, dry out, plate corrosion, general chemical breakdown etc. during and after the battery operations, which provide evidence that the PI embedded TFTCs and SU8 2000.5 adhesive are suitable materials to be placed inside the battery. Measurements show similar temperature characteristics obtained from accelerated rate calorimeter (ARC) meter [20–22], while the experimental setup is much simpler. More studies will be carried out to investigate the long term effect of the sensor materials to the performance and life time of the battery in order to realize continuous monitoring if implemented in BMS.

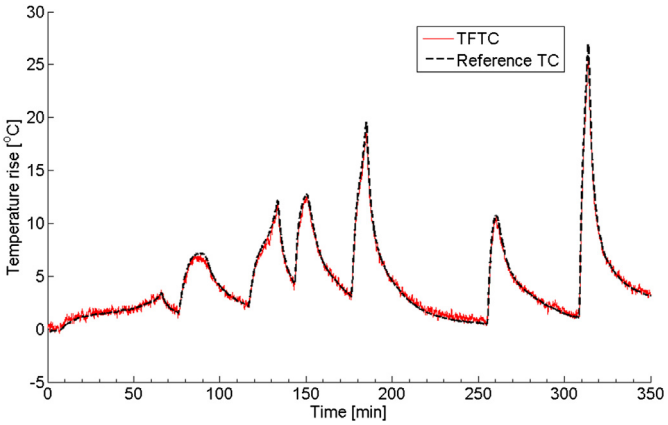

Fig. 8. Temperature profile measured from TFTC (solid) and Reference TC (dashed).

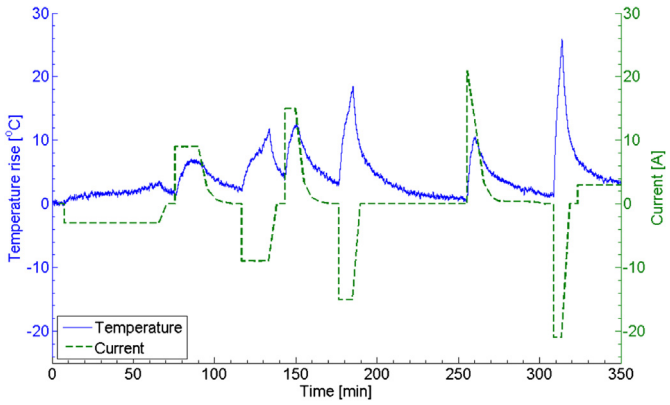

Fig. 9. Current and temperature profile when discharging and charging the cell at step-increased C-rates.

6. Conclusion

In this paper, fabrication and transfer of polyimide embedded temperature sensors from glass substrates to thin copper foils is presented. Polyimide embedded sensors adhered to the copper foils makes the sensing system, flexible, non-delicate and conductive to heat. The sensor was conveniently assembled into a pouch cell LIB in dry room with the sensor electrode pads hanging out. The temperature of the LIB was reliably measured at different charge and discharge cycles. Heat generation rate is semi-quantitatively related to the measured temperature rise profile proving that the heat generation rate inside the battery is dominant during high rate of discharge conditions. Measurements show similar temperature characteristics obtained from accelerated rate calorimeter (ARC) meter. This developed technique holds promise in realizing *in-situ* monitoring of individual cells if incorporated with battery management systems. The temperature history data obtained *in-situ* during the battery operation can help refine battery design and provide benchmark to ongoing researches on thermal modeling and simulations of lithium ion battery cells. This novel release and transfer of flexible micro sensors can be applied to other situations when sensor layers need to be conformally bonded to a flexible or freeform body.

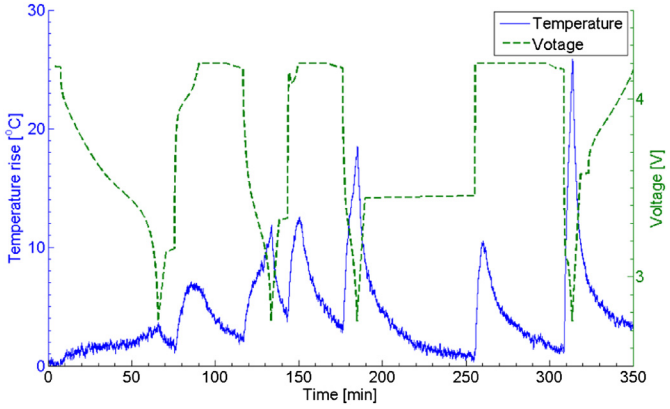

Fig. 10. Voltage and temperature profile when discharging and charging the cell at step-increased C-rates.

Acknowledgment

The financial support and technical assistance from Johnson Controls Inc. are gratefully acknowledged.

References

[1] T.M. Bandhauer, S. Garimella, T.F. Fuller, J. Electrochem. Soc. 158 (2011) R1–R25.
[2] P.G. Balakrishnan, R. Ramesh, T.P. Kumar, J. Power Sources 155 (2006) 401–414.
[3] J.W. Wen, Y. Yu, C.H. Chen, Mater. Express 2 (2012) 197–212.
[4] R. Srinivasan, B.G. Carkhuff, M.H. Butler, A.C. Baisden, Electrochim. Acta 56 (2011) 6198–6204.
[5] M.W. Verbrugge, AIChE J. 41 (1995) 1550–1562.
[6] C. Forgez, D.V. Do, G. Friedrich, M. Morcrette, C. Delacourt, J. Power Sources 195 (2010) 2961–2968.
[7] S. Al Hallaj, H. Maleki, J.S. Hong, J.R. Selman, J. Power Sources 83 (1999) 1–8.
[8] D.H. Doughty, P.C. Butler, R.G. Jungst, E.P. Roth, J. Power Sources 110 (2002) 357–363.
[9] S.C. Chen, C.C. Wan, Y.Y. Wang, J. Power Sources 140 (2005) 111–124.
[10] Imke Krüger, Martin Sievers, Gerhard Schmitz, in: Proceedings of the 7th International Modelica Conference, Como, Italy, 20–22 September 2009, Linköping University Electronic Press, Linköpings universitet, Como, Italy, 2009, pp. 1–8.
[11] R. Srinivasan, B.G. Carkhuff, A.C. Baisden, M.H. Butler, in: Proc. SPIE, International Society for Optics and Photonics, 2013, p. 87280E.
[12] R. Srinivasan, J. Power Sources 198 (2012) 351–358.
[13] J.P. Schmidt, S. Arnold, A. Loges, D. Werner, T. Wetzel, E. Ivers-Tiffée, J. Power Sources 243 (2013) 110–117.
[14] L.H.J. Raijmakers, D.L. Danilov, J.P.M. van Lammeren, M.J.G. Lammers, P.H.L. Notten, J. Power Sources 247 (2014) 539–544.
[15] C.Y. Lee, S.J. Lee, M.S. Tang, P.C. Chen, Sensors 11 (2011) 9942–9950.
[16] C.-Y. Lee, S.-J. Lee, Y.-M. Lee, M.-S. Tang, P.-C. Chen, Y.-M. Chang, in: 2012 7th IEEE International Conference on Nano/Micro Engineered and Molecular Systems (NEMS), IEEE, 2012, pp. 698–701.
[17] C.Y. Lee, S.J. Lee, Y.H. Chen, M.Y. Chung, K.C. Han, Y.M. Chang, M.S. Tang, Int. J. Electrochem. Sci. 8 (2013) 2968–2976.
[18] Z. Li, J. Zhang, B. Wu, J. Huang, Z. Nie, Y. Sun, F. An, N. Wu, J. Power Sources 241 (2013) 536–553.
[19] D. Suleiman-Rosado, J.A. Hinkley, High. Perform. Polym. 14 (2002) 317–323.
[20] J.S. Hong, H. Maleki, S. Al Hallaj, L. Redey, J. Selman, J. Electrochem. Soc. 145 (1998) 1489–1501.
[21] A. Eddahech, O. Briat, J.-M. Vinassa, in: 2013 IEEE International Symposium on Industrial Electronics (ISIE), IEEE, 2013, pp. 1–5.
[22] S. Al Hallaj, J. Prakash, J.R. Selman, J. Power Sources 87 (2000) 186–194.